^{18}F-Fluoromisonidazole PET Uptake Is Correlated with Hypoxia-Inducible Factor-1α Expression in Oral Squamous Cell Carcinoma

Jun Sato[1], Yoshimasa Kitagawa[1], Yutaka Yamazaki[1], Hironobu Hata[1], Shozo Okamoto[2], Tohru Shiga[2], Masanobu Shindoh[3], Yuji Kuge[4], and Nagara Tamaki[2]

[1]Oral Diagnosis and Medicine, Department of Oral Pathobiological Science, Graduate School of Dental Medicine, Hokkaido University, Hokkaido, Japan; [2]Department of Nuclear Medicine, Graduate School of Medicine, Hokkaido University, Hokkaido, Japan; [3]Oral Pathology and Biology, Department of Oral Pathobiological Science, Graduate School of Dental Medicine, Hokkaido University, Hokkaido, Japan; and [4]Central Institute of Isotope Science, Hokkaido University, Hokkaido, Japan

Hypoxia is a common feature of cancer and a prognostic factor for many types of cancer. ^{18}F-fluoromisonidazole (^{18}F-FMISO) PET can detect tumor hypoxia noninvasively. Hypoxia-inducible factor-1 (HIF-1) is a key player in the transcriptional response to low oxygen tension in many types of cancer. Its activity is mainly dependent on the stability and modification of HIF-1α, which is a composition of HIF-1. However, it is unclear whether ^{18}F-FMISO PET can identify HIF-1α expression in oral squamous cell carcinoma (OSCC). The present study was performed to elucidate the correlation between ^{18}F-FMISO PET findings and HIF-1α expression in OSCC. **Methods:** Twenty-three patients (age range, 42–84 y; 15 men, 8 women) with OSCC were enrolled in this study. The T-stages of cancer were T1 in 1 patient, T2 in 9, T3 in 2, and T4a in 11. The N-stages were N0 in 13 patients, N1 in 5, and N2 in 5. Each patient underwent ^{18}F-FMISO and ^{18}F-FDG PET before surgery, and the maximum standardized uptake value (SUV_{max}) of both PET studies was measured. HIF-1α expression in the operation materials was evaluated by immunohistochemical staining. The SUV_{max} of both PET studies and HIF-1α findings were compared statistically. **Results:** ^{18}F-FMISO PET detected uptake in the primary site in 14 of the 23 patients (61%). The median SUV_{max} of ^{18}F-FMISO and ^{18}F-FDG PET in the primary site was 1.83 (range, 0.8–2.7) and 16.5 (range, 1.0–32.3), respectively. There was a weak significant correlation between ^{18}F-FMISO and ^{18}F-FDG PET SUV_{max} ($P = 0.02$, $r = 0.48$). HIF-1α expression was clearly detected in 11 of the 23 patients (48%). The ^{18}F-FMISO PET SUV_{max} was significantly higher in the HIF-1α–positive cases than in the HIF-1α–negative cases (median, 2.1; range, 1.5–2.4, vs. median, 1.6; range, 0.8–2.0, respectively) ($P = 0.002$). However, there were no significant correlations between ^{18}F-FDG PET SUV_{max} and HIF-1α expression (median, 21.8; range, 7.7–29.1 vs. 1.0–32.2) ($P = 0.06$). **Conclusion:** ^{18}F-FMISO uptake in the primary site of OSCC indicates a hypoxic environment with HIF-1α expression.

Key Words: hypoxia; FMISO PET; HIF-1α; oral squamous cell carcinoma

J Nucl Med 2013; 54:1060–1065
DOI: 10.2967/jnumed.112.114355

Hypoxia is a common feature of cancer and thus is a prognostic factor for many types of cancer (*1,2*). Clinically, the prognosis of cancer with low oxygenation levels is poor, and there is strong evidence that this is due to the effects of hypoxia on therapy resistance and malignant progression (*2*). In particular, it is clear that hypoxia is a negative factor in the treatment of head and neck cancers, reducing the chance of cure (*1*). However, it is difficult to determine the conditions of hypoxia in solid tumors.

^{18}F-FDG PET is frequently used for the diagnosis and evaluation of treatment outcomes for several tumors. Multiple radiotracers have been developed for hypoxia imaging (*1*). ^{18}F-fluoromisonidazole (^{18}F-FMISO) PET is a promising noninvasive method of measuring hypoxia (*3–6*). This method is sensitive to the presence of hypoxia in viable cells and can cover the entire region of interest (*7,8*). Our recent study demonstrated high reproducibility of tumor hypoxia evaluated by ^{18}F-FMISO PET for head and neck cancer (*9*).

Hypoxia achieves many of its effects through the activation of the transcription factor hypoxia-inducible factor-1 (HIF-1) (*10*). HIF-1 is recognized as a key player in the transcriptional response to hypoxia (*11–13*). HIF-1 is a heterodimer composed of an α-subunit (HIF-1α) and a β-subunit (HIF-1β), and its activity is mainly dependent on the stability and modification of HIF-1α, the expression of which is highly regulated (*10,12*). In the case of HIF-1α, its synthesis is regulated via O_2-independent mechanisms, whereas its degradation is regulated primarily via O_2-dependent mechanisms (*10*). The heterodimer HIF-1 binds to its cognate enhancer sequence, the hypoxia-responsive element, and induces the expression of various genes responsible for the adaptation of cellular metabolism to hypoxia (the switch from oxidative respiration to anoxic respiration) (*14*), escape from hypoxia (invasion and metastasis of cancer cells) (*15*), and improvement of hypoxia (angiogenesis) (*10,16*). Because HIF-1 activity depends on HIF-1α expression level (*17*), the visualization of HIF-1α expression provides useful information on the tumor microenvironment (*17*).

Received Sep. 28, 2012; revision accepted Jan. 31, 2013.
For correspondence or reprints contact: Jun Sato, Oral Diagnosis and Medicine, Department of Oral Pathobiological Science, Hokkaido University Graduate School of Dental Medicine, North 13, West 7, Kita-ku, Sapporo 060-8586, Japan.
E-mail: jun-s@den.hokudai.ac.jp
Published online May 22, 2013.

Thus, HIF-1α overexpression may affect the prognosis of cancer patients. HIF-1α expression in oral squamous cell carcinoma (OSCC) has been shown in several recent studies (*11,13,18–21*). HIF-1α expression has been shown to correlate with poor prognosis and is an aggressive index of OSCC (*19,22,23*). Although both ^{18}F-FMISO PET and HIF-1α are important factors for hypoxia evaluation in cancer, there have been no previous reports regarding the correlation between ^{18}F-FMISO PET findings and HIF-1α expression in patients with OSCC. Therefore, the present study was performed to elucidate the correlation between ^{18}F-FMISO PET uptake and HIF-1α expression in patients with OSCC. Imaging and targeting of hypoxic cells using ^{18}F-FMISO PET and HIF-1α expression are becoming more important (*17*).

MATERIALS AND METHODS

Patients

Twenty-three consecutive patients (15 men, 8 women; median age, 67 y; age range, 42–84 y) with untreated primary OSCC undergoing medical examination and radical surgery for OSCC between October 2009 and October 2011 in our department at Hokkaido University Hospital were enrolled in this study (Table 1). None of the patients received palliative treatment. The primary tumor sites were the tongue ($n = 5$), upper gingiva ($n = 6$), lower gingiva ($n = 9$), buccal mucosa ($n = 1$), and oral floor ($n = 2$). One tumor (4%) was classified as T1, 9 (39%) as T2, 2 (9%) as T3, and 11 (48%) as T4a. The N-classifications were N0 in 13 patients (57%), N1 in 5 (21%), and N2 in 5 (22%) (*24*).

Intraoperative materials were evaluated histopathologically by hematoxylin and eosin staining and examined by 2 specialists in oral pathology masked to the specimen origin. The degree of histologic differentiation was determined in accordance with the criteria of the World Health Organization published in 1997. Of the 23 tumors, 9 (39%) were classified as grade 1, 6 (26%) as grade 2, 4 (17%) as grade 3, and 4 (17%) as unclear (*25*). The histologic mode of invasion of cancer was classified according to the Yamamoto and Kohama (YK) classification system (*26*), with YK-1 tumors having well-defined borders and YK-4 tumors having diffuse growth or invasion. Of the 23 tumors, 1 (4%) was classified as YK-1, 6 (26%) as YK-2, 11 (48%) as YK-3, 1 (4%) as YK-4, and 4 as unclear.

The protocol of this study was approved by the Institutional Review Board of Hokkaido University Hospital (2009). All the patients signed a written informed consent.

^{18}F-FMISO and ^{18}F-FDG PET Imaging

After giving their written informed consent, all the patients underwent ^{18}F-FMISO and ^{18}F-FDG PET imaging before surgery. For ^{18}F-FMISO PET, 10-min static PET images were acquired in 3-dimensional mode using an ET/CT scanner (True Point Biograph 64 with true V option; Asahi-Siemens) 4 h after the injection of 400 MBq of ^{18}F-FMISO. For ^{18}F-FDG PET, the same scanning protocol as for ^{18}F-FMISO PET was applied. At 1 h after the injection of ^{18}F-FDG (4.5 MBq/kg), the energy window was 425–650 keV, the transaxial field of view was 216 mm, and the reconstruction matrix was 168 × 168. Images were reconstructed using the iterative TrueX reconstruction method, which included partial-volume correction. The spatial resolution was 6.7 mm after reconstruction (*9*). The detailed methods of ^{18}F-FMISO PET and high reproducibility of tumor hypoxia evaluated by ^{18}F-FMISO PET for head and neck cancer in our institution have been described in our recent study (*9*).

For the semiquantitative evaluation of both ^{18}F-FMISO and ^{18}F-FDG uptake in the primary tumor, the highest uptake in the tumor was estimated using a maximum standardized uptake value (SUV_{max}).

PET images were evaluated by specialists in nuclear medicine masked to the clinical information for each case. The patients underwent

TABLE 1
Patients in This Study

Patient no.	Age (y)	Sex	Classification		Primary site	^{18}F-FMISO uptake	^{18}F-FMISO PET SUV_{max}	^{18}F-FDG PET SUV_{max}	HIF-1α
			T	N					
1	65	M	4a	1	Upper gingiva	−	1.39	30.05	−
2	62	M	4a	0	Upper gingiva	+	1.57	12.20	+
3	62	M	3	2	Tongue	+	2.06	17.90	+
4	79	F	2	0	Lower gingiva	−	1.46	5.90	−
5	72	M	4a	0	Upper gingiva	+	1.32	2.99	−
6	56	F	4a	0	Upper gingiva	−	1.74	9.40	−
7	65	M	2	1	Lower gingiva	+	2.10	21.43	+
8	73	F	2	2	Lower gingiva	−	1.64	4.00	−
9	57	M	4a	0	Oral floor	+	1.98	32.20	−
10	59	M	4a	2	Oral floor	+	2.19	29.10	+
11	83	F	2	0	Lower gingiva	+	2.16	7.70	+
12	70	F	2	0	Lower gingiva	−	1.72	9.90	+
13	59	F	4a	1	Tongue	+	2.40	21.80	+
14	67	M	4a	0	Lower gingiva	+	1.59	16.60	−
15	64	M	4a	0	Lower gingiva	+	2.02	13.10	−
16	70	M	2	1	Tongue	+	2.06	25.50	+
17	59	F	3	0	Tongue	+	1.53	16.50	−
18	79	F	1	0	Upper gingiva	−	0.84	6.50	−
19	79	F	4a	2	Upper gingiva	+	2.73	23.40	+
20	74	M	2	0	Buccal mucosa	−	1.83	7.40	−
21	42	M	2	2	Tongue	−	1.83	1.00	−
22	71	M	4a	1	Lower gingiva	+	2.40	22.90	+
23	84	M	2	1	Lower gingiva	+	1.82	12.60	+

^{18}F-FMISO and ^{18}F-FDG PET on different days. Therefore, the nuclear medicine specialists also evaluated each image independently on different days. When necessary, they referred to enhanced CT images to confirm the tumor region. The average and median of the interval of both PET studies were 3.1 ± 3.7 d and 1 d (range, 1–16 d), respectively.

Immunohistochemical Study for HIF-1α

The immunohistochemical detection of HIF-1α was conducted using formalin-fixed paraffin-embedded tissue sections. The sections were deparaffinized, rehydrated, and immersed in 3% hydrogen peroxide in distilled water for 5 min to block endogenous peroxidase activity. They were incubated with a primary mouse monoclonal antibody to HIF-1α (sc-13515, 1:100 dilution; Santa Cruz Biotechnology) overnight at 4°C. The epitope of this antibody is mapped within amino acids 329–530 of HIF-1α of human origin, and the antibody has no cross-reactivity to HIF-2α or HIF-3α. After being washed with phosphate-buffered saline, the sections were stained with Simple Stain MAX–PO (Nichirei Biosciences) for 30 min and visualized with Envision Plus Kits/HRP (Dako) at room temperature. The peroxidase reaction products were developed with 3,3′-diaminobenzidine, and the sections were counterstained with hematoxylin. Negative controls in which the primary antibody was replaced with normal rat IgG were run with each specimen. HIF-1α positivity was evaluated by counting positive cells among 500–1,000 tumor cells at a magnification of ×200 in 3 different areas. We set the cutoff value of HIF-1α–positive cells at 5% of the positively stained cells (*21*). This work was performed by 2 of the authors who were masked to the identities of the patients from whom the specimens had been obtained.

Statistical Analysis

A Spearman correlation coefficient was used to compare the relationship between the SUV_{max} of ^{18}F-FMISO and of ^{18}F-FDG PET. The Mann–Whitney *U* test was used to compare the SUV_{max} of ^{18}F-FMISO and of ^{18}F-FDG PET in patients with and without HIF-1α expression. In the same way, the Mann–Whitney *U* test, χ^2 test, and logistic regression analysis were used to compare SUV_{max} or HIF-1α expression and other factors, including patient age, T- and N-classifications, degree of histologic differentiation, and histologic mode of invasion. The factors assessed included sex, T-classification (T1 + 2 vs. T3 + 4), N-classification (N0 vs. N1 + 2), degree of histologic differentiation (grade 1 vs. grade 2 + 3), and mode of invasion (YK-1 + 2 vs. YK-3 + 4). All statistical analyses were performed using Stat View J-5.0 statistical software (Abacus Concepts). In all analyses, a *P* value of less than 0.05 was taken to indicate statistical significance.

RESULTS

^{18}F-FMISO and ^{18}F-FDG PET Imaging

^{18}F-FMISO and ^{18}F-FDG PET detected uptake in primary sites of OSCC in 14 (61%) and 22 (96%) of the 23 patients, respectively (Fig. 1). Only 1 patient (patient 21) showed no ^{18}F-FDG uptake. The median SUV_{max} of ^{18}F-FMISO and ^{18}F-FDG PET in the primary site was 1.83 (range, 0.8–2.7) and 16.5 (range, 1.0–32.3), respectively (Table 1; Figs. 1–3).

The weak correlation between ^{18}F-FMISO and ^{18}F-FDG SUV_{max} was statistically significant ($P = 0.02$, $r = 0.48$) (Fig. 1). However, if we delete 2 extreme data points of ^{18}F-FMISO SUV_{max} (patients 18 and 19) from the analysis, the correlation is not significant ($P = 0.06$, $r = 0.41$; data not shown).

Immunohistochemical Staining for HIF-1α and PET Imaging

The immunohistochemical staining of HIF-1α was performed on 23 cases of squamous cell carcinoma in the oral region. Positive signals were observed in 11 of the 23 cases (48%) (Table 1; Figs. 2 and 3). HIF-1α was detected in the cytoplasm and nucleus of cancer cells (Fig. 2). No obvious signals of HIF-1α were observed in normal stromal cells around the cancer parenchyma and negative-control specimens (data not shown).

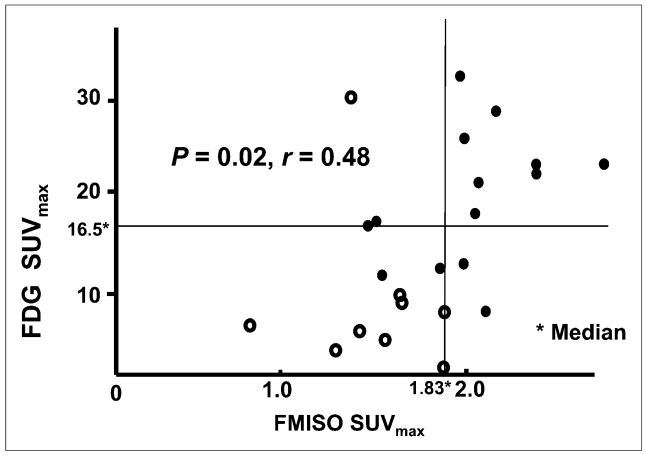

FIGURE 1. Relationship of SUV_{max} between ^{18}F-FMISO and ^{18}F-FDG PET. There was weak significant correlation in SUV_{max} between ^{18}F-FMISO and ^{18}F-FDG PET by Spearman correlation coefficient ($P = 0.02$, $r = 0.48$). Median SUV_{max} of ^{18}F-FMISO and ^{18}F-FDG PET was 1.83 and 16.5, respectively. ○ = results of cases without ^{18}F-FMISO uptake.

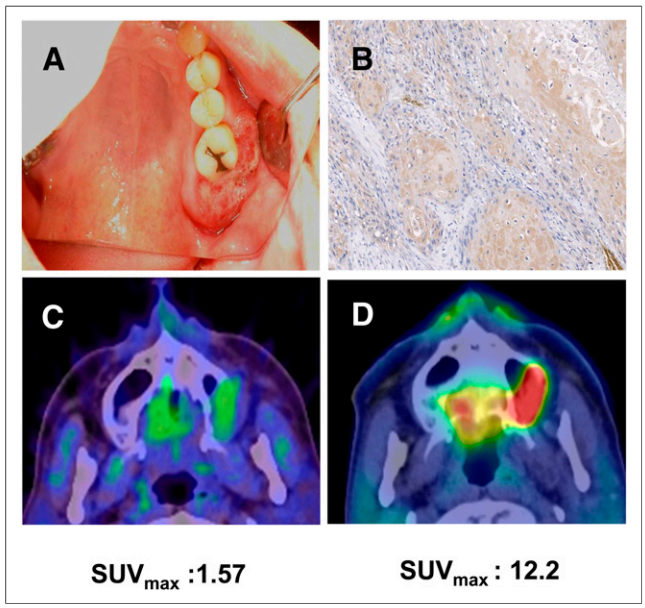

FIGURE 2. Clinical findings, ^{18}F-FMISO and ^{18}F-FDG PET images, and immunohistochemical staining of HIF-1α for patient 2. (A) Case of left upper gingival squamous cell carcinoma. Tumor can be seen in left upper maxillary region. (B) For ^{18}F-FMISO PET, definite uptake was detected in left maxillary primary site of cancer (SUV_{max}, 1.57). (C) For ^{18}F-FDG PET, definite uptake was also seen in left maxillary primary site of cancer (SUV_{max}, 12.2). (D) HIF-1α expression was detected in nucleus and cytoplasm of cancer cells by immunohistochemical analysis.

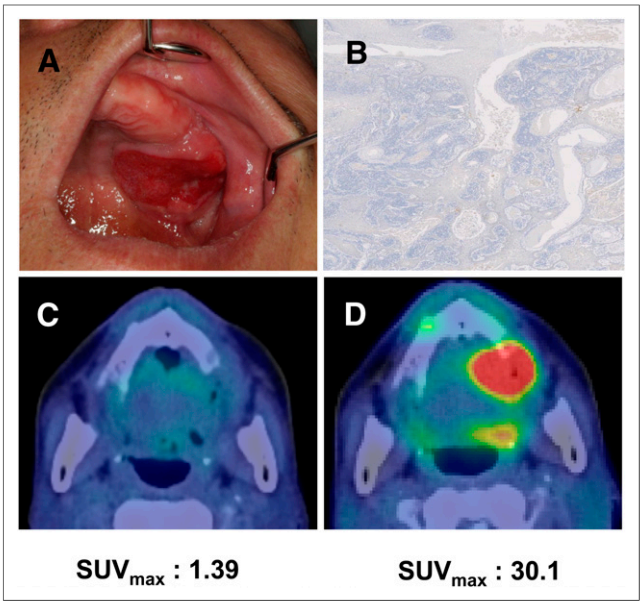

FIGURE 3. Clinical findings, ^{18}F-FMISO and ^{18}F-FDG PET images, and immunohistochemical staining of HIF-1α for patient 1. (A) Case of left upper gingival SCC. Tumor can be seen in left upper maxillary region. (B) For ^{18}F-FMISO PET, definite uptake was not detected in primary site of cancer (SUV_{max}, 1.39). (C) For ^{18}F-FDG PET, definite uptake was detected in primary site of cancer (SUV_{max}, 30.1). (D) Weak HIF-1α expression was observed in cancer cells by immunohistochemical analysis.

The prevalence of HIF-1α positivity was significantly higher in patients with ^{18}F-FMISO uptake in primary sites than in those without uptake (10/14 vs. 1/9; $P < 0.005$) (Table 2). The SUV_{max} of ^{18}F-FMISO PET was significantly higher in patients positive for HIF-1α than in those negative for HIF-1α (median, 2.1; range, 1.5–2.4, vs. median, 1.6; range, 0.8–2.0 [$P = 0.002$]) (Fig. 4). If we delete 2 extreme data points of ^{18}F-FMISO SUV_{max} (patients 18 and 19) from the analysis, the correlation is still significant ($P = 0.006$; data not shown). However, there were no significant correlations between the SUV_{max} of ^{18}F-FDG PET and HIF-1α (median, 21.8; range, 7.7–29.1, vs. median, 8.4; range, 1.0–32.2 [$P = 0.06$]) (Fig. 5).

As for the correlations of SUV_{max} with clinical findings, there was no significant correlation between ^{18}F-FMISO PET SUV_{max} and age of the patients ($P = 0.29$) (data not shown), T-classification ($P > 0.99$) (Fig. 6), N-classification ($P = 0.14$) (data not shown), degree of histologic differentiation ($P = 0.51$) (data not shown), or histologic mode of invasion ($P = 0.52$) (data not shown).

DISCUSSION

The results of the present study indicated a significant correlation between ^{18}F-FMISO uptake and HIF-1α expression in patients with OSCC. Our results confirmed that ^{18}F-FMISO uptake indicates the presence of hypoxic areas in a tumor with a high degree of confidence.

Hypoxia is characteristic of solid tumors arising from a less ordered vasculature and necrosis (*20,27,28*). Hypoxia can also induce major changes in gene expression, thereby enhancing the metastatic ability of tumor cells (*1*). Therefore, intratumoral hypoxia is one of the most important mechanisms promoting tumor aggressiveness, metastasis, and poor prognosis (*11*). Consequently, the noninvasive imaging of HIF-1α expression and activity is of great interest because it may be useful for predicting cancer prognosis (*29*). Thus, the significant association observed between ^{18}F-FMISO uptake and HIF-1α expression in patients with OSCC is an important finding of the present study.

^{18}F-FMISO PET, showing specific uptake in hypoxic tissue, is a promising noninvasive method of measuring hypoxia (*4–6*). Eschmann et al. (*3*) performed ^{18}F-FMISO PET for 14 cases of advanced head and neck cancers and reported that before radiotherapy all the patients showed enhanced ^{18}F-FMISO uptake throughout the entire tumor area. Moreover, they found a correlation between the SUV_{max} of ^{18}F-FMISO PET and tumor recurrence, because both are linked to hypoxia. In the present study, 14 of the 23 patients (61%) showed ^{18}F-FMISO uptake in primary sites of OSCC. However, 9 patients showed no definite ^{18}F-FMISO uptake in such primary sites. This observation may be explained by differences between the characteristics of the patients; in the study by Eschmann et al. (*3*), only 4 of the 14 patients had OSCC (29%). In oral lesions, metal artifacts due to dental restoration may also decrease image quality. ^{18}F-FMISO PET images typically have low signal-to-noise characteristics, and metal artifacts may easily decrease image quality (*7*).

Some recent studies have shown that HIF-1–active regions are heterogeneous (*30,31*). Kudo et al. revealed that HIF-1α expression is not ubiquitous but heterogeneous and is small in tumors (*30*). On the other hand, Fillies et al. (*21*) found that in most cases, HIF-1α expression did not vary much among the tumor cores of each individual patient, indicating a rather homogeneous HIF-1α expression throughout the tumor in patients with oral floor cancer. A recent study has indicated that HIF-1 expression supports the adaptation of hypoxic cancer cells by inducing the expression of genes related to glucose metabolism and glucose transport, producing angiogenic and growth factors that help improve the nutritional environment, and preventing death by apoptosis (*17*). These chain-of-survival actions are linked to the malignancy change of

TABLE 2
Relationship Between ^{18}F-FMISO Uptake and HIF-1α Expression

Uptake	Cases		
	HIF-1α positivity	HIF-1α negativity	Total
^{18}F-FMISO (positive)	10	4	14
^{18}F-FMISO (negative)	1	8	9
Total	11	12	23

10/14 vs. 1/9; $\chi^2 = 8.0$; $P < 0.005$.

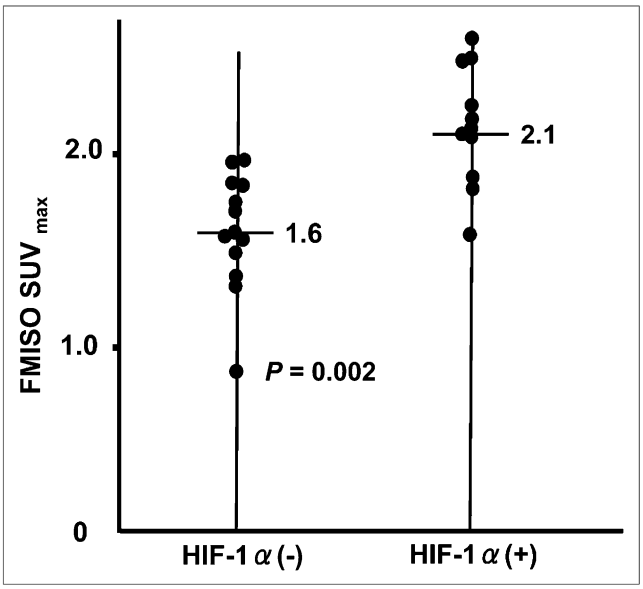

FIGURE 4. Relationship between ^{18}F-FMISO SUV_{max} and HIF-1α expression. SUV_{max} of ^{18}F-FMISO was significantly higher in HIF-1α–positive cases than in HIF-1α–negative cases ($P = 0.002$, Mann–Whitney *U* test). Bars indicate median of SUV_{max}.

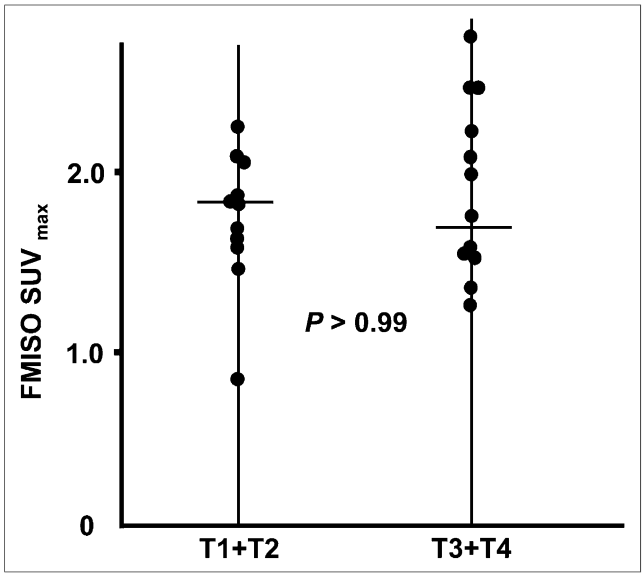

FIGURE 6. Relationship between ^{18}F-FMISO SUV_{max} and T-classification. There was no significant correlation between ^{18}F-FMISO PET SUV_{max} and T-classification ($P > 0.99$, Mann–Whitney *U* test). Bars indicate median of SUV_{max}.

the entire cancer (*17*). These findings suggest that the HIF-1 action affects the malignancy of the entire tumor, regardless of whether or not the HIF-1α expression is heterogeneous.

Although there have been some immunohistochemical studies of HIF-1α (*21,32,33*), the literature gives no uniform recommendation for a cutoff point of HIF-1α expression. Beasley et al. (*34*) used a cutoff value of greater than 1% in oral cancer. Other authors used cutoff values between 1% and 5% (*21,33*). In this study, we set the cutoff value at 5% of the HIF-1α–positive cells in accordance with the study of Fillies et al. (*21*), who demonstrated that the 5% HIF-1α expression threshold can be used to distinguish 2 different populations with significant statistical differences in survival prognosis.

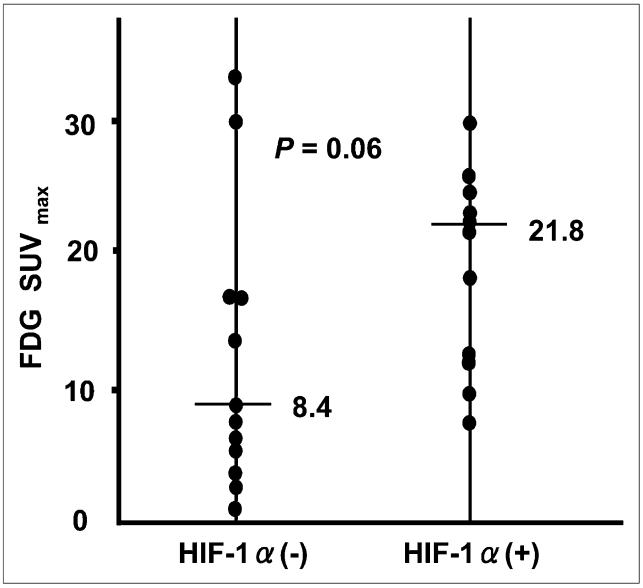

FIGURE 5. Relationship between ^{18}F-FDG SUV_{max} and HIF-1α expression. There was no significant correlation between ^{18}F-FDG PET SUV_{max} and HIF-1α expression ($P = 0.06$, Mann–Whitney *U* test). Bars indicate median of SUV_{max}.

The direct measurement of tumor partial oxygen pressure (pO_2) can be made using an Eppendorf electrode. Tumor hypoxia is usually identified by pO_2 values less than or equal to 10 mm Hg; whereas normal tissues have pO_2 values of 24–66 mm Hg (*1,2*). ^{18}F-FMISO uptake increases only when the pO_2 value falls below 2–3 mm Hg (*29*). A previous immunohistochemical study showed that HIF-1α is more frequently observed adjacent to blood vessels than in pimonidazole-positive regions (*29*) and that the pO_2 values in HIF-1–active regions are approximately 10–15 mm Hg (*29,35*). This result suggests that ^{18}F-FMISO uptake reflects more severe hypoxic conditions than the region of HIF-1α expression. Moreover, this finding suggests that there are some discrepancies between the regions of ^{18}F-FMISO uptake and HIF-1α expression. However, in the present study, we could not compare definite locations between ^{18}F-FMISO uptake and HIF-1α expression, because the specialists in oral pathology and nuclear medicine evaluated HIF-1α expression and PET images independently.

In the present study, there was no significant correlation between ^{18}F-FDG uptake and HIF-1α expression. This finding suggests that ^{18}F-FMISO uptake and HIF-1α expression indicate not only increased glucose metabolism, but also hypoxia.

The major limitation of this study was the small patient population used. Moreover, the distributions of both ^{18}F-FMISO uptake and HIF-1α expression in cancer could not be accurately determined. Further studies using a larger number of cases are required to address these issues.

In addition, in the present study, we could demonstrate HIF-1α expression in the hypoxic region of a tumor evaluated by ^{18}F-FMISO PET. However, we could not elucidate the function and activity of HIF-1, a heterodimer composed of HIF-1α and HIF-1β, in OSCC in the present study. The correlation between HIF-1 activity and ^{18}F-FMISO uptake is important for understanding

the microenvironment of OSCC and for planning a strategy for OSCC treatment. Examining this correlation is the next target of our research.

HIF-1 was initially identified because of its response to low O_2 concentrations, but it is now apparent that HIF-1 can be regulated by other factors such as oncogene activation or the loss of tumor suppression (*36*). The expression of oncogenes such as HRAS-V12 leads to the accumulation of HIF-1α under both normoxic and hypoxic conditions (*36*). To our regret, we could not provide information on the possibility of HIF-1α expression under normoxic conditions in OSCC. This is another limitation of this study.

CONCLUSION

We demonstrated that there is a significant relationship between definite ^{18}F-FMISO uptake and HIF-1α expression, which are both key features of hypoxia, in primary sites of cancer in patients with OSCC. In the future, ^{18}F-FMISO PET may be used in the decision-making process regarding treatment strategies.

DISCLOSURE

The costs of publication of this article were defrayed in part by the payment of page charges. Therefore, and solely to indicate this fact, this article is hereby marked "advertisement" in accordance with 18 USC section 1734. This study was partially supported by a grant-in-aid for scientific research (2010–2011: 22592203). No other potential conflict of interest relevant to this article was reported.

REFERENCES

1. Wang W, Lee NY, Georgi JC, et al. Pharmacokinetic analysis of hypoxia ^{18}F-fluoromisonidazole dynamic PET in head and neck cancer. *J Nucl Med.* 2010;51:37–45.
2. Janssen HL, Haustermans KM, Balm AJ, et al. Hypoxia in head and neck cancer: how much, how important? *Head Neck.* 2005;27:622–638.
3. Eschmann SM, Paulsen F, Bedeshem C, et al. Hypoxia-imaging with ^{18}F-misonidazole and PET: changes of kinetics during radiotherapy of head-and-neck cancer. *Radiother Oncol.* 2007;83:406–410.
4. Koh WJ, Rasey JS, Evans ML, et al. Imaging of tumor hypoxia in human tumors with [F-18] fluoromisonidazole. *Int J Radiat Oncol Biol Phys.* 1992;22:199–212.
5. Rasey JS, Koh WJ, Fvans ML, et al. Quantifying regional hypoxia in human tumors with positron emission tomography of [F-18] fluoromisonidazole: a pretherapy study of 37 patients. *Int J Radiat Oncol Biol Phys.* 1996;36:417–428.
6. Rajendran JG, Wilson DC, Conrad EU, et al. [^{18}F]FMISO and [^{18}F] FDG PET imaging in soft tissue sarcoma: correlation of hypoxia, metabolism and VEGF expression. *Eur J Nucl Med Mol Imaging.* 2003;30:695–704.
7. Jansen JFA, Schöder H, Lee NY, et al. Noninvasive assessment of tumor microenviroment using dynamic contrast-enhanced magnetic resonance imaging and ^{18}F-fluoromisonidazole positron emission tomography imaging in neck nodal metastases. *Int J Radiat Oncol Biol Phys.* 2010;77:1403–1410.
8. Lee ST, Scott AM. Hypoxia positron emission tomography imaging with 18-fluoromisonidazole. *Semin Nucl Med.* 2007;37:451–461.
9. Okamoto S, Shiga T, Yasuda K, et al. High reproducibility of tumor hypoxia evaluated by ^{18}F-fluoromisonidazole PET for head and neck cancer. *J Nucl Med.* 2013;54:201–207.
10. Harada H, Inoue M, Itasaka S, et al. Cancer cells that survive radiation therapy acquire HIF-1 activity and translocate towards tumour blood vessels. *Nat Commun.* 2012;3:783.
11. Nordsmark M, Bentzen S, Rudat V, et al. Prognostic value of tumor oxygenation in 397 head and neck tumors after primary radiation therapy: an international multi-center study. *Radiother Oncol.* 2005;77:18–24.
12. Semenza GL. Targeting HIF-1 for cancer therapy. *Nat Rev Cancer.* 2003;3:721–732.
13. Lin PY, Yu CH, Wang JT, et al. Expression of hypoxia-inducible factor-1α is significantly associated with the progression and prognosis of oral squamous cell carcinomas in Taiwan. *J Oral Pathol Med.* 2008;37:18–25.
14. Semenza GL. Regulation of cancer cell metabolism by hypoxia-inducible factor 1. *Semin Cancer Biol.* 2009;19:12–16.
15. Chan DA, Giaccia AJ. Hypoxia, gene expression, and metastasis. *Cancer Metastasis Rev.* 2007;26:333–339.
16. Liao D, Johnson RS. Hypoxia: a key regulator of angiogenesis in cancer. *Cancer Metastasis Rev.* 2007;26:281–290.
17. Kizaka-Kondoh S, Tanaka S, Hiraoka M. Imaging and targeting of the hypoxia-inducible factor 1-active microenvironment. *J Toxicol Pathol.* 2009;22:93–100.
18. Liang X, Zheng M, Jiang J, et al. Hypoxia-inducible factor-1 alpha, in association with TWIST2 and SNIP1, is a critical prognostic factor in patients with tongue squamous cell carcinoma. *Oral Oncol.* 2011;47:92–97.
19. Uehara M, Sano K, Ikeda H, et al. Hypoxia-inducible factor 1 alpha in oral squamous cell carcinoma and its relation to prognosis. *Oral Oncol.* 2009;45:241–246.
20. Roh JL, Cho KJ, Kwon GY, et al. The prognostic value of hypoxia markers in T2-staged oral tongue cancer. *Oral Oncol.* 2009;45:63–68.
21. Fillies T, Werkmeister R, van Diest P, et al. HIF1-alpha overexpression indicates a good prognosis in early stage squamous cell carcinoma of the oral floor. *BMC Cancer.* 2005;5:84–91.
22. Liu SY, Chang LC, Pan LF, et al. Clinicopathologic significance of tumor cell-lined vessel and microenviroment in oral squamous cell carcinoma. *Oral Oncol.* 2008;44:277–285.
23. Aebersold DM, Burri P, Beer KT, et al. Expression of hypoxia-inducible factor 1 alpha: a novel predictive and prognostic parameter in the radiotherapy of oropharyngeal cancer. *Cancer Res.* 2001;61:2911–2916.
24. Barnes L, Eveson J, Reichart P, et al. *World Health Organization Classification of Tumors, Pathology and Genetics of Tumors of the Head and Neck.* International Agency for Research on Cancer. Lyon, France: IARC Press; 2005.
25. Sobin LH, Wittenkind CH. *TNM Classification of Malignant Tumors.* 5th ed. New York, NY: John Wiley & Sons, Inc.; 1997.
26. Yamamoto E, Kohama G, Sunakawa H, et al. Mode of invasion, bleomycin sensitivity, and clinical course in squamous cell carcinoma of the oral cavity. *Cancer.* 1983;51:2175–2180.
27. Schliephake H. Prognostic relevance of molecular markers of oral cancer: a review. *Int J Oral Maxillofac Surg.* 2003;32:233–245.
28. Németh Z, Velich N, Bogdan S, et al. The prognostic role of clinical, morphological and molecular markers in oral squamous cell tumors. *Neoplasma.* 2005;52:95–102.
29. Kudo T, Ueda M, Kuge Y, et al. Imaging of HIF-1-active tumor hypoxia using a protein effectively delivered to and specifically stabilized in HIF-1-active tumor cells. *J Nucl Med.* 2009;50:942–949.
30. Kudo T, Ueda M, Konishi H. PET imaging of hypoxia-inducible factor-1 active tumor cells with pretargeted oxygen-dependent degradable streptavidin and a novel ^{18}F-Labeled biotin derivative. *Mol Imaging Biol.* 2011;13:1003–1010.
31. Krohn KA, Link JM, Mason RP. Molecular imaging of hypoxia. *J Nucl Med.* 2008;49(suppl 2):129S–148S.
32. Serganova I, Doubrovin M, Vider J, et al. Molecular imaging of temporal dynamics and spatial heterogeneity of hypoxia-inducible factor-1 signal transduction activity in tumour in living mice. *Cancer Res.* 2004;64:6101–6108.
33. Bos R, Van Der Groep P, Greijer AE, et al. Levels of hypoxia-inducible factor-1 alpha independently predict prognosis in patients with lymph node negative breast carcinoma. *Cancer.* 2003;97:1573–1581.
34. Beasley NJP, Leek R, Alam M, et al. Hypoxial-inducible factors HIF-1α and HIF-2α in head and neck cancer: relationship to tumor biology and treatment outcome in surgically resected patients. *Cancer Res.* 2002;62:2493–2497.
35. Jiang BH, Semenza GL, Bauer C, et al. Hypoxia-inducible factor 1 levels vary exponentially over a physiologically relevant range of O_2 tension. *Am J Physiol.* 1996;271:C1172–C1180.
36. Denko NC. Hypoxia, HIF1 and glucose metabolism in the solid tumor. *Nat Rev Cancer.* 2008;8:705–713.